

Theoretical Study on the Small Clusters of LiH, NaH, BeH₂, and MgH₂

Yung-Lung Chen*

Department of Chemical Engineering, WuFeng Institute of Technology, Chia-Yi, Min-Hsiung, Taiwan 621

Chun-Huei Huang and Wei-Ping Hu*

Department of Chemistry and Biochemistry, National Chung Cheng University, Chia-Yi, Min-Hsiung, Taiwan 621

Received: April 16, 2005; In Final Form: July 14, 2005

High-level ab initio molecular orbital theory is used to calculate the geometries, vibrational frequencies, atomic charges, and binding energies of the small clusters (LiH)_n, (NaH)_n, (BeH₂)_n, and (MgH₂)_n ($n = 1-4$). For (LiH)_n and (NaH)_n, there are planar cyclic structures when $n = 2, 3$. We have found the cubic structure T_d in addition to the planar cyclic D_{4h} when $n = 4$. The D_{4h} is less stable than the T_d geometry. For (BeH₂)_n and (MgH₂)_n, when $n = 3$, there are three kinds of structures: chain C_{2v} , planar cyclic D_{3h} , and hat-like C_{2v} . The C_{2v} geometry is more stable than the others. When $n = 4$, there are four kinds of structures: chain D_{2h} , cubic T_d , string-like C_2 , and cubic transformation C_1 . The most stable compounds in the families of (LiH)_n, (NaH)_n, (BeH₂)_n, and (MgH₂)_n are cubic T_d , cubic T_d , chain D_{2h} , and string-like C_2 geometries, respectively, when $n = 4$. Calculated binding energies range from -24 to -37 kcal/mol for (LiH)_n and -19 to -30 kcal/mol for (NaH)_n, (BeH₂)_n, and (MgH₂)_n. The hydrogen atoms in hydride clusters always have negative charges. The atomic charges of planar cyclic structures are weaker than those of cubic structures, and there is a tendency of reducing along with the increase of the cluster size. The vibrational frequencies of planar cyclic structures have consistent tendency, too. It indicates that the bond distance increases with the ionic character of the bond.

Introduction

Metal hydrides are used extensively as drying and reducing agents in solution chemistry.¹ The reduction potential of the H⁻/H₂ couple has been estimated as -2.25 V.² It has made the hydride anion one of the most powerful reducing agents.³⁻⁵ It is interesting for us to understand those clusters of metal hydrides, because the century of nanotechnology is coming and the computer hardware is advancing vigorously. Lithium hydride, the simplest neutral heteropolar diatomic molecule, has been the object of intense theoretical and spectroscopic study since the 1930s. Stwalley and Zemke⁶ had identified and reviewed significant experimental measurements and many theoretical calculations of the spectroscopy and structure of the isotopic lithium hydrides (⁶LiH, ⁷LiH, ⁶LiD, ⁷LiD). All of the above electronic structure calculations were nonrelativistic and also in the Born–Oppenheimer approximation, but were calculated only at the Hartree–Fock level. Shukla et al.⁷ presented an ab initio embedded-cluster approach to electronic structure calculations on crystalline solids, within the framework of the linear combination of atomic orbitals method, and described the applications of this approach to the evaluation of the ground-state energy per unit cell of the lithium hydride crystal. Bellaiche et al.⁸ calculated the directional Compton profiles and the anisotropies of Compton scattering based on the density functional theory in the local density approximation, performed in the plane-wave basis, and using full, unscreened Coulomb potentials for both Li and H atoms. They found that the influence of correlation on Compton profiles in LiH was

very weak. For cluster structures, the dimer structure forms a basis for the formation of large clusters as well as crystals; therefore, Kulkarni et al.^{9,10} took up a systematic investigation of the occurrence of dihydrogen bonds in the main group elements. The complexes of LiH, BH₃, and AlH₃ with the third-row hydrides, as well as their dimers, were studied at the ab initio MP2 level of theory and compared with the corresponding second-row hydrides. Those results made us start considering what would happen to the clusters of metal hydride, especially for the simplest alkaline metal and alkaline-earth metal. Fuentelba et al.¹¹ calculated the dipole polarizability of a series of the type Li_nH_m ($n, m \leq 4$) using density functional methods. The study of the trends in the mean polarizability and the anisotropy was explained in terms of the interplay between electronic and geometrical effects. Antoine et al.¹² studied the metastable decomposition of the hydrogenated lithium cluster ion (LiH)_nLi_m⁺ ($m = 0, 1, \text{ and } 3; n \leq 15$) by using a reflectron mass spectrometer. These clusters were found to be decomposed by evaporation of a LiH or Li₂H₂ molecule. The following year, Antoine et al.¹³ kept on studying the metallicity of lithium-rich Li_nH_m⁺ cluster ions ($1 \leq m \leq 6, n \leq 22$, and $(n - m) > 3$) by measuring unimolecular dissociation rates. These clusters were found to be decomposed by evaporation of a Li atom or a Li₂ molecule. Lithium hydrides are important as models, because they are the simplest electron-deficient ionic metal compounds. The potential of these hydrides to cluster and form multicentered bonds has been the focus of attention in the fields of chemistry. Many theoretical papers have been devoted to this item. For instance, Kato et al.¹⁴ used the ab initio theory HF/5-21G to study the structure and stability of small lithium hydrides, Li_nH_m ($m \leq n \leq 4$). They also evaluated the heats of reaction and the

* Corresponding authors. (Chen) E-mail: ylchen@mail.wfc.edu.tw. Fax: 886-5-226-4224. (Hu) E-mail: chewph@ccu.edu.tw.

TABLE 1: Calculated Bonding Energies (ΔE , in kcal/mol) of Lithium Hydride Clusters at Various Levels

	MP2/6-311G**	MP2/6-311++G**	QCISD(T)/6-311G**// MP2/6-311++G**	QCISD/6-311G**	QCISD(T)/6-311G**	QCISD(T)/ 6-311G(2df,2pd)// QCISD/6-311G**
LiH ($C_{\infty v}$)	0.00	0.00	0.00	0.00	0.00	0.00
(LiH) ₂ (D_{2h})	-24.60	-24.59	-24.54	-24.43	-24.54	-24.36
(LiH) ₃ (D_{3h})	-32.63	-32.61	-32.60	-32.48	-32.60	-32.16
(LiH) ₄ (D_{4h})	-35.13	-35.12	-35.07	-34.97	-35.07	-34.58
(LiH) ₄ (T_d)	-37.04	-37.02	-37.23	-36.94	-37.23	-36.69

appearance potentials and compared those with the experimental mass spectroscopic results. Kollman et al.¹⁵ used electronic structure calculations to predict the existence and the properties of the lithium hydride dimer. They had computed the vibrational frequencies, the quadrupole moment, and the thermodynamic functions. Their analysis of geometry, charge redistribution, and molecular orbital energy shifts in the linear and cyclic dimer reveals interesting similarities to previous work, but their computations were only at the Hartree–Fock level. So, if the monomer number increased, or the metal was changed, what trends will there be for the geometries and atomic charges of the clusters? Dill et al.¹⁶ examined a systematic set of 33 neutral molecules and complexes that contain lithium or beryllium and another heavy atom. They investigated the ionic, multicentered, and coordinate bonding. These included singly bonded, doubly bonded, hydrogen-bridged metal complexes, and coordinate donor–acceptor complexes. Therefore, we shall want to understand how the clusters are bonded. Cardelino et al.¹⁷ used ab initio theory to study all possible molecules and monovalent cations containing lithium and hydrogen, up to a total of 4 atoms. They analyzed the stabilities and structures of lithium clusters and hydrides, both neutral and positively charged, formed by 4 or fewer atoms, but those were calculated only at the Hartree–Fock self-consistent field (SCF) molecular orbital theory. Rao et al.¹⁸ used the self-consistent-field-linear-combination-of-atomic-orbitals-molecular-orbital method (SCF-LCAO-MO) to calculate equilibrium geometries, binding energies, and stability of metal clusters, Li and Y, containing hydrogen atoms. Bonačić-Koutecký et al.¹⁹ used ab initio methods to study structural and optical response properties of stoichiometric small Li_nH_n and nonstoichiometric Li_nH_m ($n - m = 1, 2, 3, 8$) clusters containing single and multiple excess electrons. Fuentealba and Savin²⁰ used the electron localization function to study the bonding characteristics of the hydrogenated clusters Li_4H_n ($n = 0-4$). Abdurahman et al.²¹ reported the ab initio electronic structure calculations of the polymeric lithium hydride chain $(LiH)_\infty$ and beryllium hydride chain $(Be_2H_4)_\infty$. Vezin et al.²² compared optical absorption spectra of Li_4H and Li_9H clusters that had been recorded by depletion spectroscopy in the visible range with ab initio calculation results of both clusters. For BeH_2 , Brendel et al.²³ first prepared the crystalline beryllium hydride. The gaseous BeH_2 molecule had not been synthesized until 2002 by Bernath et al.²⁴ With only 6 electrons, BeH_2 is a favorite target molecule for testing new ab initio methods.²⁵⁻²⁸ However, less research of the hydrides NaH and MgH_2 was carried out.

The metal hydride clusters of LiH, BeH_2 , NaH, and MgH_2 span a wide range of structural types. Structures of these hydrides thus involve multicentered electron-deficient, coordinate, ionic, and covalent bonding. However, there is no research in studying these hydride chemistries systematically. We begin with these small cluster systems in order to investigate the geometries, bonding energies, atomic charges, and vibrational frequencies systematically.

Methods

The molecular geometries of the clusters of LiH, NaH, BeH_2 , and MgH_2 were calculated by using MP2²⁹ theory with the 6-311G** and 6-311++G** basis sets and by using QCISD^{30,31} theory with the 6-311G** basis set. To obtain more accurate energies, single-point energies were also calculated by using QCISD(T)^{30,31} theory with the 6-311G** and 6-311G(2df,2pd) basis sets at the MP2/6-311++G** and QCISD/6-311G** geometries, respectively. The harmonic vibrational frequencies were calculated by using MP2 theory with the 6-311++G** basis set. The ChelpG atomic charges were calculated by using QCISD theory with the 6-311G** basis set.

For LiH clusters, to figure out the effects of high-level theory on geometry optimizations and the diffuse functions on metal and hydrogen atoms, we also employed QCISD(T)/6-311G** and MP2/6-311++G** to calculate geometry optimizations. To search accurate geometry and understand the effects of model theory and basis sets on geometry optimizations, we also used MP2, QCISD, and QCISD(T) theory with 6-31G**, 6-31++G**, 6-311G**, 6-311++G**, 6-311G(2df,2pd), and 6-311++G-(2df,2pd) basis sets to calculate the geometries and frequencies of linear LiH and NaH clusters. The calculations were carried out by using the *Gaussian 98* program³² on several Linux workstations in our theoretical chemistry laboratory.

Results and Discussion

1. Bonding Energy and Geometry. LiH Clusters. Table 1 shows the calculated bonding energies of the clusters $(LiH)_n$ ($n = 1-4$) at various theoretical levels. Figure 1 shows the calculated geometries at MP2/6-311++G** and QCISD/6-311G** levels. The bonding energy, ΔE , is defined as the classical (or Born–Oppenheimer) energy change of the following reactions per molar monomer (MH or $M'H_2$):



Here, M is the Li or Na atom, and M' is the Be or Mg atom. There are planar cyclic structures where $n = 2-4$. We also find the cubic structure T_d in addition to the planar D_{4h} for $n = 4$. The bonding energy of the cubic structure T_d is predicted to be -36.69 kcal/mol at the highest level in the current study. The calculation also shows that the D_{4h} is less stable by 2.11 kcal/mol than the T_d geometry. By increasing the size of the basis set from 6-31G** to 6-311G**, the differences of the calculated bonding energies are only about 0.72 kcal/mol. By adding diffuse functions to heavy atoms and hydrogen, the differences of the calculated bonding energies are only about 0.02 and 0.07 kcal/mol, respectively. By increasing the number of the polarization functions from (d,p) to (2df,2pd), the differences of the calculated bonding energies are only about 0.39 kcal/mol. All employed computational methods find the bonding

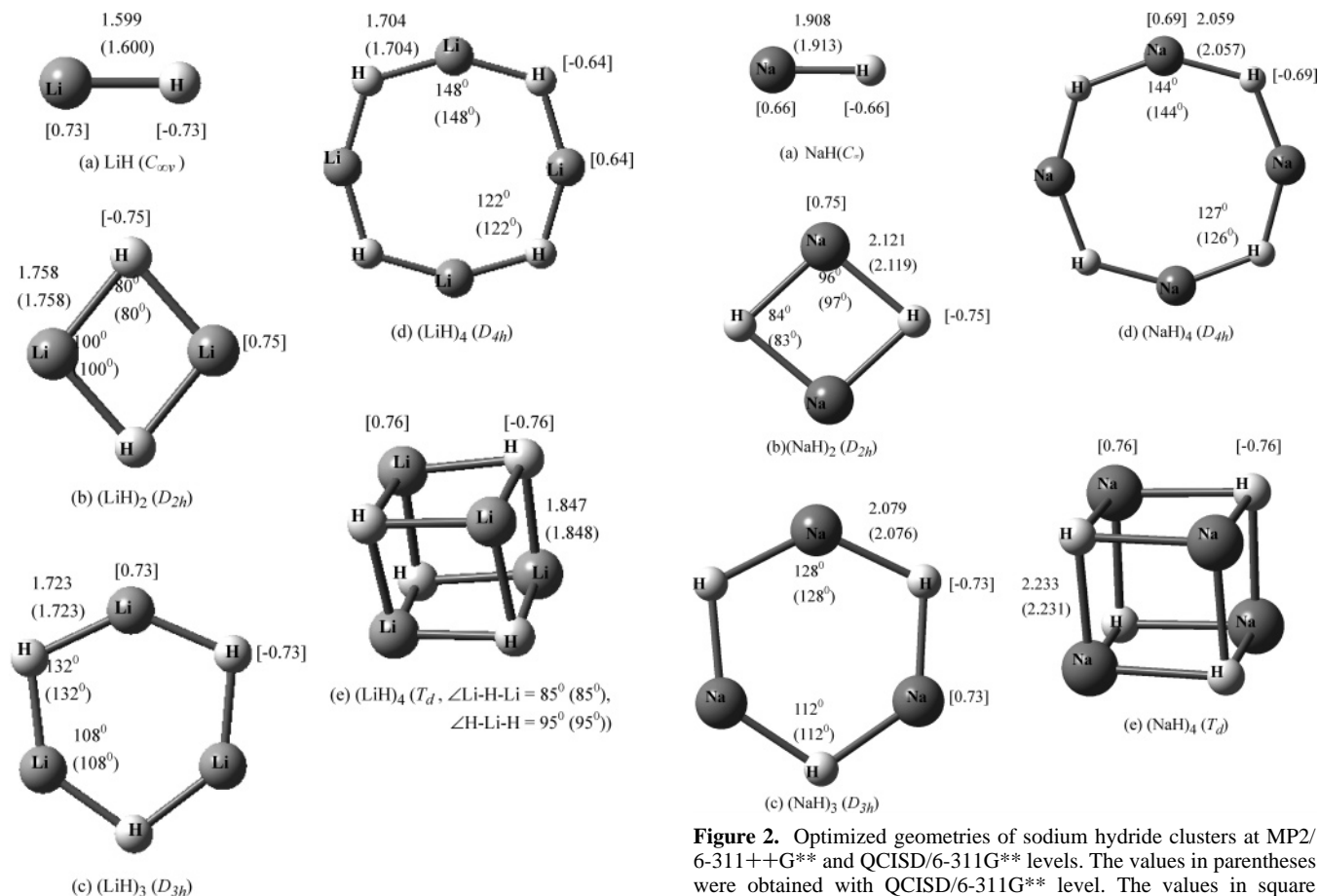


Figure 1. Optimized geometries of lithium hydride clusters at MP2/6-311++G** and QCISD/6-311G** levels. The values in parentheses were obtained with QCISD/6-311G** level. The values in square brackets were ChelpG atomic charges. The bond lengths are in angstroms, angles in degrees.

energies to be similar. It is shown that these geometries have converged, and the calculated results must be accurate and reliable.

Now, let us consider some features of the optimized geometrical parameters. The geometries of lithium hydride clusters optimized by the energy gradient method are schematically described in Figure 1 together with bond distances. The experimental bond length of gaseous LiH is 1.595 Å,¹⁴ and the crystalline is 2.05 Å.³⁴ The previous theoretical studies of LiH were 1.516,¹⁶ 1.608,³⁷ 1.62,³⁸ 1.633,¹⁵ and 1.638 Å,³³ but they were calculated only at the Hartree–Fock level. It was found that the results tended to yield either longer bond lengths or shorter than the experimental values, and the difference was about 0.013–0.079 Å. LiH is linear $C_{\infty v}$ geometry, and the bond length is 1.600 Å at the QCISD/6-311G** level in the current study. It is well-established that the MP2/6-311++G** method will produce geometries that are quite similar to the QCISD/6-311G** calculated geometries, and both are very close to the experimental geometry. The difference between the present work

Figure 2. Optimized geometries of sodium hydride clusters at MP2/6-311++G** and QCISD/6-311G** levels. The values in parentheses were obtained with QCISD/6-311G** level. The values in square brackets were ChelpG atomic charges. The bond lengths are in angstroms, angles in degrees.

and the experimental value is the smallest when it is compared to the other previous theoretical work above. For the planar cyclic lithium hydrides clusters considered here, there are two cationic Li atoms surrounding each anionic H atom, namely, tricentered bonds. The bond distance decreases as the size of the clusters increases from $n = 2$ to $n = 4$, but the differences are only about 0.019–0.054 Å. For the three-dimensional T_d geometry of (LiH)₄, the distance becomes greater than the corresponding distance of the D_{4h} . In this case, there are three cationic Li atoms surrounding each anionic H atom, namely, tetracentered bonds. That is to say, the bond distance increases with the coordinate numbers, because the structural type of the clusters is varied from tricentered to tetracentered bonding.

We also examine the correlation between binding energy and bond distance for the planar cyclic lithium hydride clusters. The bond distance decreases as the size of the clusters increases from $n = 2$ to $n = 4$, and the tendency of the binding energies is the same as that of the bond distance. It indicates that the bond strength increases with cluster size.

NaH Clusters. Table 2 shows the calculated bonding energies of the clusters (NaH)_{*n*} ($n = 1-4$) at various theoretical levels. Figure 2 shows the calculated geometries at MP2/6-311++G**

TABLE 2: Calculated Bonding Energies (ΔE , in kcal/mol) of Sodium Hydride Clusters at Various Levels

	MP2/6-311G**	MP2/6-311++G**	QCISD(T)/6-311G**// MP2/6311++G**	QCISD/6-311G**	QCISD(T)/6-311G(2df,2pd)// QCISD/6-311G**
NaH ($C_{\infty v}$)	0.00	0.00	0.00	0.00	0.00
(NaH) ₂ (D_{2h})	-19.40	-19.38	-18.81	-16.17	-19.00
(NaH) ₃ (D_{3h})	-26.89	-26.85	-26.31	-23.67	-26.23
(NaH) ₄ (D_{4h})	-29.20	-29.17	-28.57	-25.95	-28.52
(NaH) ₄ (T_d)	-30.14	-30.10	-29.68	-26.94	-29.54

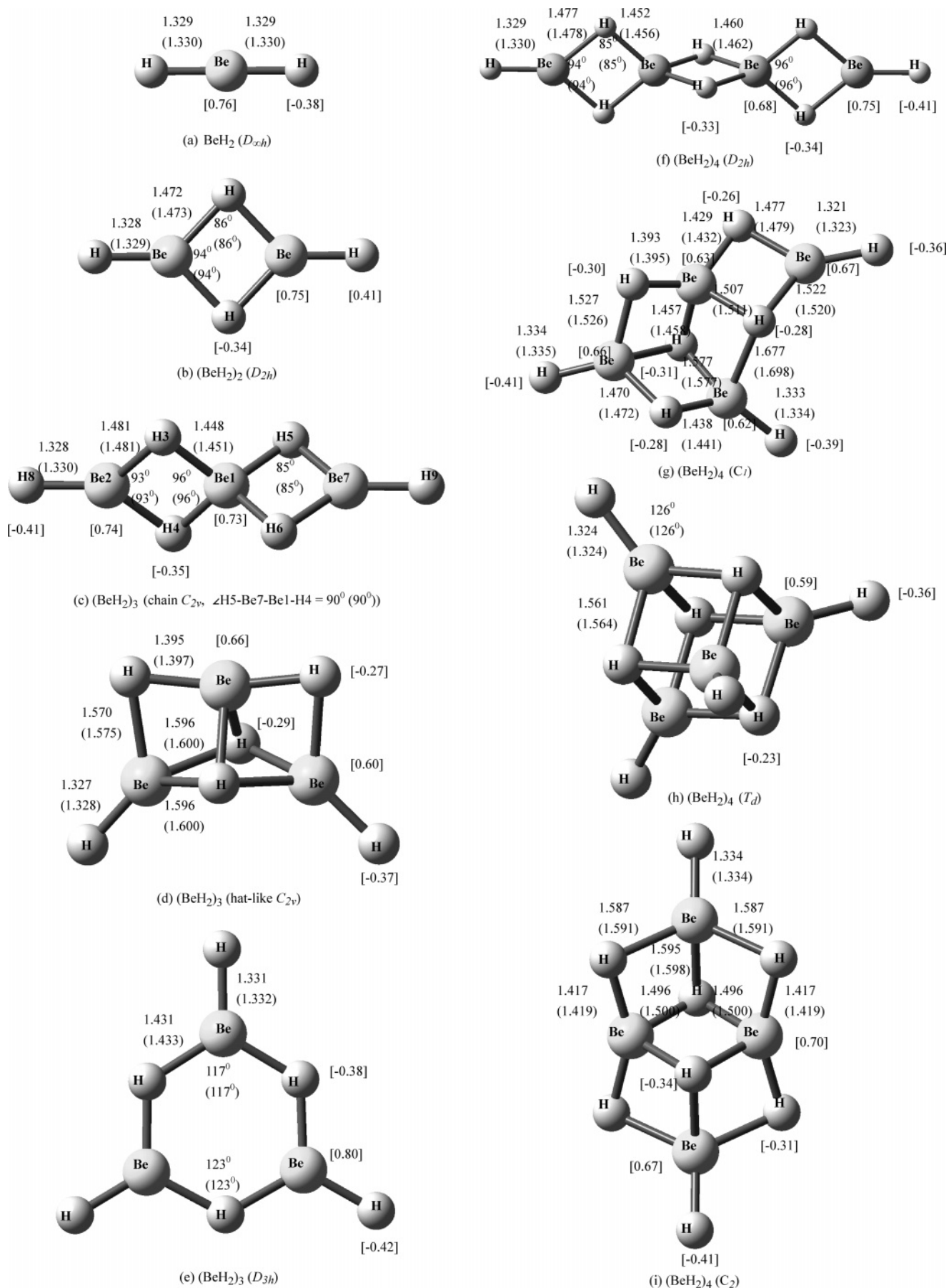


Figure 3. Optimized geometries of beryllium hydride clusters at MP2/6-311++G** and QCISD/6-311G** levels. The values in parentheses were obtained with QCISD/6-311G** level. The values in square brackets were ChelpG atomic charges. The bond lengths are in angstroms, angles in degrees.

TABLE 3: Calculated Bonding Energies (ΔE , in kcal/mol) of Beryllium Hydride Clusters at Various Levels

	MP2/6-311G**	MP2/6-311++G**	QCISD(T)/6-311G**// MP2/6-311++G**	QCISD/6-311G**	QCISD(T)/6-311G(2df,2pd)// QCISD/6-311G**
BeH ₂ (<i>D</i> _{∞h})	0.00	0.00	0.00	0.00	0.00
(BeH ₂) ₂ (<i>D</i> _{2h})	-16.14	-16.13	-16.35	-15.98	-16.83
(BeH ₂) ₃ (<i>D</i> _{3h})	-16.96	-16.96	-17.23	-16.80	-17.86
(BeH ₂) ₃ (hat-like <i>C</i> _{2v})	-22.02	-22.02	-22.26	-21.37	-23.03
(BeH ₂) ₃ (chain <i>C</i> _{2v})	-24.29	-24.28	-24.53	-23.97	-25.24
(BeH ₂) ₄ (<i>T</i> _d)	-22.98	-23.00	-23.33	-22.42	-23.97
(BeH ₂) ₄ (<i>C</i> ₁)	-24.47	-24.50	-24.79	-23.99	-25.57
(BeH ₂) ₄ (<i>C</i> ₂)	-25.60	-25.64	-25.87	-24.93	-26.87
(BeH ₂) ₄ (<i>D</i> _{2h})	-28.07	-28.07	-28.32	-27.67	-29.14

TABLE 4: Calculated Bonding Energies (ΔE , in kcal/mol) of Magnesium Hydride Clusters at Various Levels

	MP2/6-311G**	MP2/6-311++G**	QCISD(T)/6-311G**// MP2/6-311++G**	QCISD/6-311G**	QCISD(T)/6-311G(2df,2pd)// QCISD/6-311G**
MgH ₂ (<i>D</i> _{∞h})	0.00	0.00	0.00	0.00	0.00
(MgH ₂) ₂ (<i>D</i> _{2h})	-16.07	-16.05	-16.12	-15.95	-16.60
(MgH ₂) ₃ (<i>D</i> _{3h})	-20.59	-20.58	-20.60	-20.41	-21.08
(MgH ₂) ₃ (hat-like <i>C</i> _{2v})	-20.56	-20.54	-20.84	-20.41	-21.54
(MgH ₂) ₃ (chain <i>C</i> _{2v})	-22.36	-22.35	-22.41	-22.17	-23.11
(MgH ₂) ₄ (<i>C</i> _{2v})	-21.08	-21.07	-21.02	-20.84	-21.66
(MgH ₂) ₄ (<i>T</i> _d)	-24.63	-24.60	-25.00	-24.54	-25.43
(MgH ₂) ₄ (<i>C</i> ₁)	-24.70	-24.71	-24.91	-24.53	-25.53
(MgH ₂) ₄ (<i>C</i> ₂)	-26.83	-26.84	-27.05	-26.62	-27.80
(MgH ₂) ₄ (<i>D</i> _{2h})	-25.46	-25.46	-25.51	-25.24	-26.30

and QCISD/6-311G** levels. There are planar cyclic structures when $n = 2-4$. We also find the cubic structure *T*_d in addition to the planar *D*_{4h} for $n = 4$. The bonding energy of the cubic structure *T*_d is predicted to be -29.54 kcal/mol at the highest level in the current study. The calculation also shows that the *D*_{4h} is less stable by 1.02 kcal/mol than the *T*_d geometry. The effects of the basis set size, diffuse functions, and the number of the polarization functions on these clusters are similar to those of lithium hydride clusters. All employed computational methods find the bonding energies to be similar. It is shown that these geometries have converged, and the calculated results must be accurate and reliable compared to those of lithium hydride clusters.

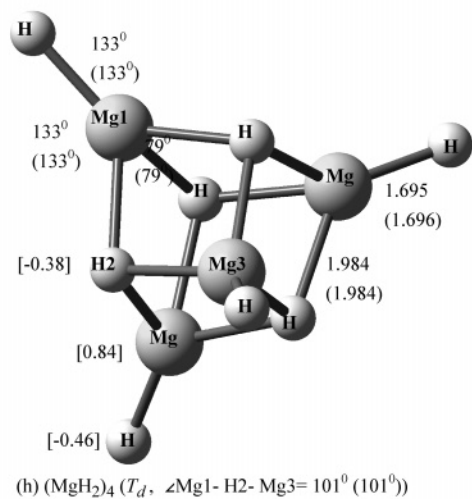
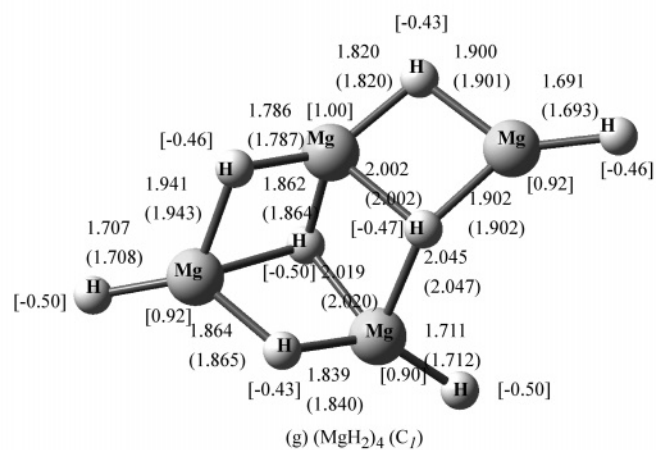
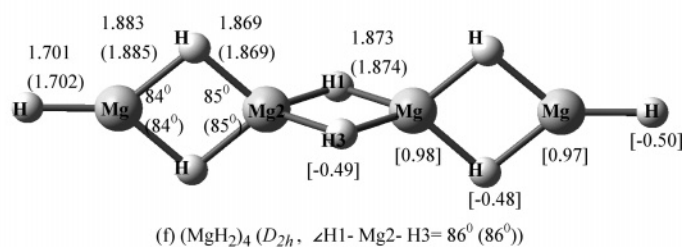
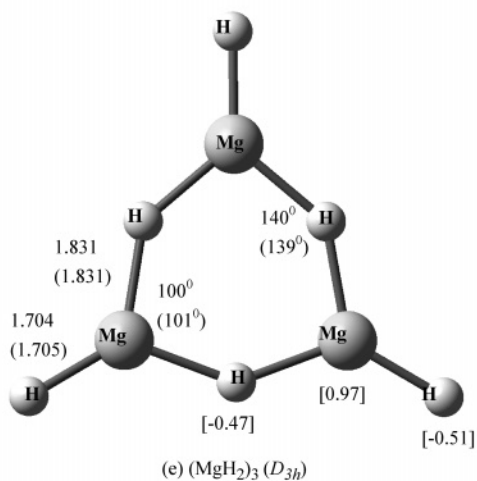
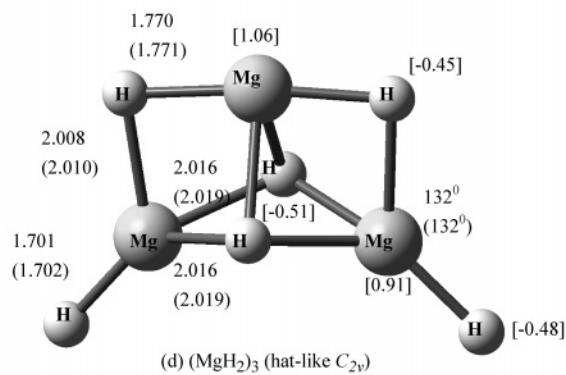
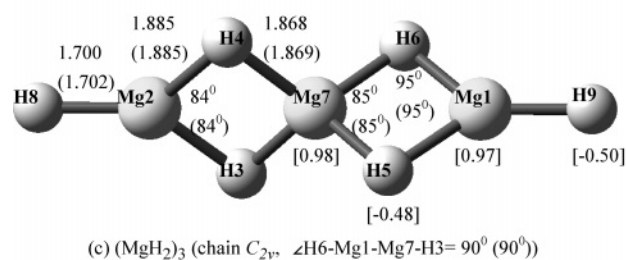
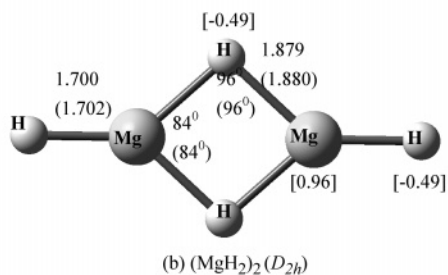
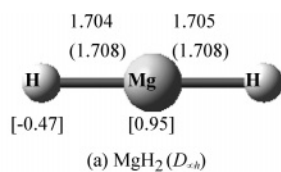
The geometries of sodium hydride clusters are schematically described in Figure 2 together with bond distances. The experimental bond length of crystalline NaH is 2.44 Å.³⁵ NaH is linear *C*_{∞v} structure, and the bond length is 1.913 Å at the QCISD/6-311G** level in the present study. It is apparent that the MP2/6-311++G** method will produce geometries that are quite similar to the QCISD/6-311G** calculated geometries. For the planar cyclic sodium hydride clusters considered here, there are two cationic Na atoms surrounding each anionic H atom, namely, tricentered bonds. The bond distance decreases as the cluster size increases from $n = 2$ to $n = 4$, but the difference is only about 0.019–0.062 Å. For the three-dimensional *T*_d geometry of (NaH)₄, the distance becomes greater than the corresponding distance of the *D*_{4h}. In this case, there are three cationic Na atoms surrounding each anionic H atom, namely, tetracentered bonds. That is to say, the bond distance increases with the coordinate numbers because the structural types of clusters are varied from tricentered to tetracentered bonding. We also examine the correlation between binding energy and bond distance for the planar cyclic sodium hydride clusters. The bond distance decreases as the size of the clusters increases from $n = 2$ to $n = 4$, and the tendency of the binding energies is the same as that of the bond distance. It indicates that the bond strength increases with the size of the clusters.

BeH₂ Clusters. Table 3 shows the calculated bonding energies of the clusters (BeH₂)_{*n*} ($n = 1-4$) at various theoretical levels.

Figure 3 shows the calculated geometries at MP2/6-311++G** and QCISD/6-311G** levels. When $n = 3$, there are three kinds of structures: chain *C*_{2v}, hat-like *C*_{2v}, and planar cyclic *D*_{3h}. The bonding energy of the chain *C*_{2v} geometry is predicted to be -25.24 kcal/mol at the highest level in the current study, and it is more stable by 2.21–7.38 kcal/mol than the others. When $n = 4$, there are four kinds of structures, chain *D*_{2h}, string-like *C*₂, cubic transformation *C*₁, and cubic *T*_d. The bonding energy of the *D*_{2h} geometry is predicted to be -29.14 kcal/mol at the highest level in the current study. The calculation also shows that the *D*_{2h} geometry is more stable by 2.27–5.17 kcal/mol than the others. The effects of the basis set size, diffuse functions, and the number of the polarization functions on these clusters are not apparent, which is similar to lithium hydride clusters. All employed computational methods find the bonding energies to be similar. It is shown that these geometries have converged, and the calculated results must be accurate and reliable as those of lithium hydride clusters.

The geometries of beryllium hydride clusters are schematically described in Figure 3 together with bond distances. The experimental bond length of gaseous BeH₂ is 1.333 761 Å.²⁴ BeH₂ is linear *D*_{∞h} structure, and the bond length is 1.330 Å at the QCISD/6-311G** level in the present study. It is apparent that the MP2/6-311++G** method will produce geometries that are quite similar to the QCISD/6-311G** calculated geometries, and both are very similar to the experimental geometry. By increasing cluster size, the bond length of the tail ends of the cluster is almost changeless and about 1.3 Å, but from end to center, we find that the bond length is not regular.

MgH₂ Clusters. Table 4 shows the calculated bonding energies of the clusters (MgH₂)_{*n*} ($n = 1-4$) at various theoretical levels. Figure 4 shows the calculated geometries at MP2/6-311++G** and QCISD/6-311G** levels. When $n = 3$, there are three kinds of structures: chain *C*_{2v}, hat-like *C*_{2v}, and planar cyclic *D*_{3h}. The bonding energy of the chain *C*_{2v} geometry is predicted to be -23.11 kcal/mol at the highest level in the current study, and it is more stable than the others about 1.57–2.03 kcal/mol. When $n = 4$, there are four kinds of structures as beryllium hydride clusters: chain *D*_{2h}, string-like *C*₂, cubic transformation *C*₁, and cubic *T*_d. We also find a ring-like *C*_{2v}



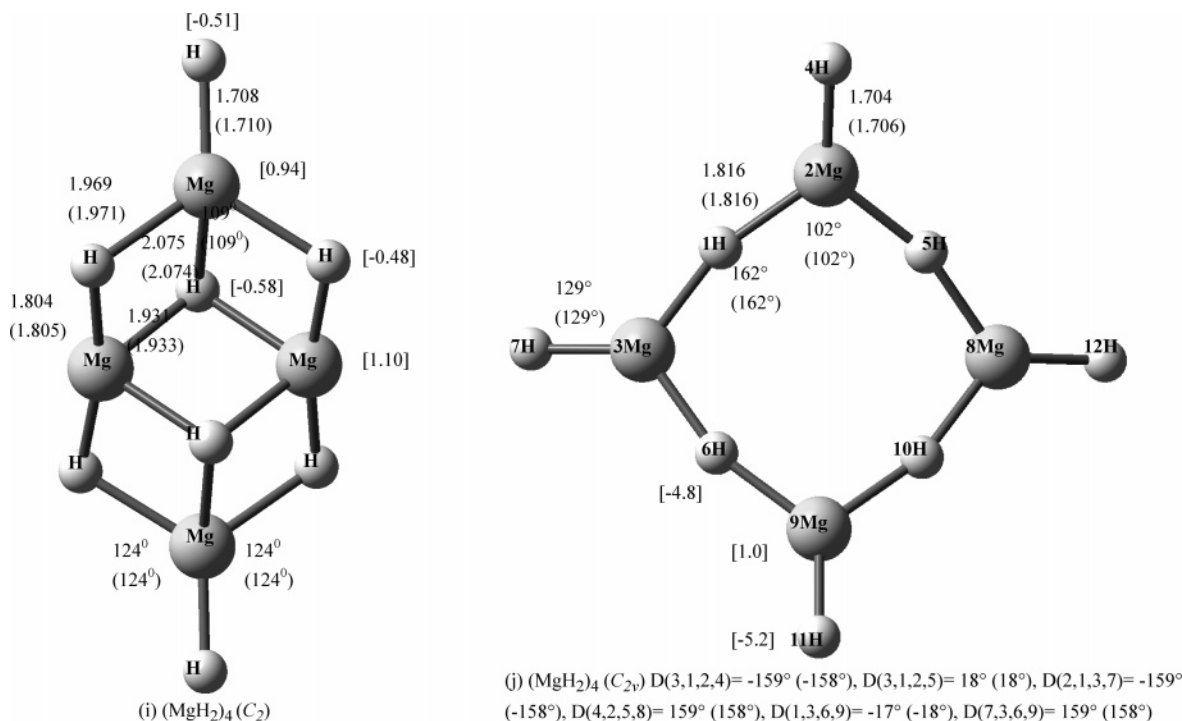


Figure 4. Optimized geometries of magnesium hydride clusters at MP2/6-311++G** and QCISD/6-311G** levels. The values in parentheses were obtained with QCISD/6-311G** level. The values in square brackets were ChelpG atomic charges. The bond lengths are in angstroms, angles in degrees. D is dihedral angle.

in addition to these four kinds of structures. The bonding energies of the D_{2h} , C_1 , and T_d are similar. The differences of these bonding energies are only about 0.87 kcal/mol. The calculation also shows that the C_2 geometry is more stable by 1.50–6.14 kcal/mol than the others. The effects of the basis set size, diffuse functions, and the number of the polarization functions on these clusters are not apparent, which is similar to lithium hydride clusters. All employed computational methods find the bonding energies to be similar. It is shown that these geometries have converged, and the calculated results must be accurate and reliable as those of lithium hydride clusters.

The geometries of magnesium hydride clusters are schematically described in Figure 4 together with bond distances. The experimental bond length of crystalline MgH_2 is 1.95 Å.³⁶ MgH_2 is linear $D_{\infty h}$ structure, and the bond length is 1.708 Å at the QCISD/6-311G** level in the present study. It is apparent that the MP2/6-311++G** method will produce geometries that are quite similar to those of the QCISD/6-311G** calculated geometries, and the difference of the bond distance is only about 0.004 Å (angle is 1°). By increasing the size of the cluster, the bond length of the tail ends of the cluster is almost changeless and about 1.7 Å, but from the end to the center, we find that the bond length is not regular.

Comparison Between Hydrides with Different Metals. When we compared LiH with NaH clusters, we found the effects of the basis set size, diffuse functions, and the number of the polarization functions on these two kinds of clusters were similar. The trends of these effects on BeH_2 and MgH_2 clusters were the same. When we compared the bonding energies of LiH with NaH clusters, the calculation showed that the LiH clusters were more stable by 5–7 kcal/mol than the NaH clusters. The differences of bonding energies for BeH_2 and MgH_2 clusters were not apparent, although BeH_2 were a little stable than MgH_2 clusters, too. When we compared LiH with BeH_2 clusters, we found the bonding energies of LiH clusters were more stable by ~ 8 kcal/mol than the BeH_2 clusters. But the bonding energies of NaH clusters were more stable only by

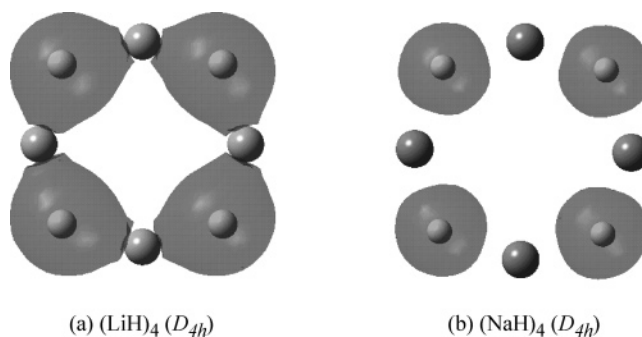


Figure 5. Calculated electron density isosurface (0.01 au) of $(\text{LiH})_4$ and $(\text{NaH})_4$ at QCISD/6-311G** level.

~ 3 kcal/mol than the those of the MgH_2 clusters. Therefore, we can suggest that the stability decreases as the metal atom size increases from Li to Na (or Be to Mg) and as the metal atomic number increases from Li to Be (or Na to Mg).

2. Atomic Charges. LiH and NaH Clusters. The atomic charges of lithium hydride and sodium hydride clusters are given in Figures 1 and 2, respectively. The hydrogen atoms in hydride clusters always have negative charges. This implies that the hydrogen atom always behaves as the electronegative species toward the lithium and sodium atoms. For example, the calculated electron density isosurfaces of $(\text{LiH})_4$ and $(\text{NaH})_4$ are shown in Figure 5. We could find a noticeable difference in the electron density between Li and H atoms. For the planar cyclic hydride clusters considered here, there are two cationic Li (or Na) atoms surrounding each anionic H atom. The atomic charges decrease as the size of the clusters increases from $n = 2$ to $n = 4$. On the other hand, the ionic character of the bond decreases as the size of the clusters increases. For the three-dimensional T_d structures of $(\text{LiH})_4$ and $(\text{NaH})_4$, there are three cationic Li (or Na) atoms surrounding each anionic H atom. The atomic charges of planar cyclic structures (D_{2h} , D_{3h} , and D_{4h}) are weaker than those of cubic structures (T_d). That is to say, the ionic character increases with the coordinate numbers

TABLE 5: Frequencies (cm^{-1}) of Lithium Hydride Clusters at MP2/6-311++G Level**

LiH	(LiH) ₂ (<i>D</i> _{2h})	(LiH) ₃ (<i>D</i> _{3h})	(LiH) ₄ (<i>D</i> _{4h})	(LiH) ₄ (<i>T</i> _d)
1432	1194	1249	1395	1108
	1091	1249	1395	979
	985	1231	1380	979
	902	1012	1364	979
	604	946	879	953
	524	946	870	953
		596	823	953
		416	823	930
		328	568	930
		328	396	717
		264	396	717
		264	332	717
			307	520
			307	392
			211	392
			176	392
			118	373
			112	373

of atom. We also examine the correlation between atomic charges and bond distance. It indicates that the bond distance increases with the ionic character of the bond. Thus, the Li–H (or Na–H) distance depends mainly on the ionic character of the bond.

BeH₂ and MgH₂ Clusters. The atomic charges of beryllium hydride and magnesium hydride clusters are given in Figures 3 and 4, respectively. The hydrogen atoms in hydride clusters always have negative charges as LiH and NaH clusters do above. This implies that the hydrogen atom always behaves as the electronegative species toward the beryllium and magnesium atoms. For the planar cyclic hydride clusters considered here (*D*_{2h} and *D*_{3h} geometries when $n = 2$ and 3, respectively), there are two cationic Be (or Mg) atoms surrounding one anionic H atom, namely, tricentered bonds, for some H atoms. The atomic charges of these H atoms increase from -0.34 to -0.38 when the size of the clusters increases from $n = 2$ to $n = 3$. These are different from those of the LiH and NaH clusters. For the three-dimensional *T_d* structures of (BeH₂)₄ and (MgH₂)₄, there are three cationic Be (or Mg) atoms surrounding one anionic H atom, namely, tetracentered bonds, for some H atoms. The atomic charges of the tricentered bonds of the planar cyclic structures are stronger than those of the tetracentered bonds of the cubic structures (*T_d*). These are also different from those of the LiH and NaH clusters above.

Comparison Between Hydrides with Different Metals. When we compared LiH with NaH clusters, we found that the difference in the atomic charges was not apparent, but there was more difference between BeH₂ and MgH₂ clusters. The atomic charges of the MgH₂ clusters were stronger than those of the BeH₂ clusters.

3. Frequencies. We used MP2 theory with the 6-311++G** basis set to calculate the harmonic vibrational frequencies of these hydride clusters. Tables 5–8 show the calculated frequencies of the lithium hydride, sodium hydride, beryllium hydride, and magnesium hydride clusters, respectively. In Table 5, for the planar cyclic clusters of lithium hydride considered here, we had found that the stretch vibrational modes of Li–H at higher-frequency parts had divided into two sections (higher and lower frequencies). That is to say, for (LiH)₂ at higher-frequency parts, there were two $\sim 1100 \text{ cm}^{-1}$ higher-frequency modes and two $\sim 950 \text{ cm}^{-1}$ lower-frequency modes. For (LiH)₃ at higher-frequency parts, there were three $\sim 1200 \text{ cm}^{-1}$ higher-frequency modes and three $\sim 1000 \text{ cm}^{-1}$ lower-frequency modes. For (LiH)₄ at higher-frequency parts, there were four

TABLE 6: Frequencies (cm^{-1}) of Sodium Hydride Clusters at MP2/6-311++G Level**

NaH	(NaH) ₂ (<i>D</i> _{2h})	(NaH) ₃ (<i>D</i> _{3h})	(NaH) ₄ (<i>D</i> _{4h})	(NaH) ₄ (<i>T</i> _d)
1182	993	1046	1159	918
	855	1046	1138	822
	823	965	1138	822
	690	821	1079	822
	458	720	712	757
	228	720	632	757
		455	632	743
		251	606	743
		251	442	743
		186	310	549
		116	310	549
		116	181	549
			153	239
			140	172
			140	172
			87	172
			51	160
			47	160

$\sim 1400 \text{ cm}^{-1}$ higher-frequency modes and four $\sim 900 \text{ cm}^{-1}$ lower-frequency modes. We also had found that the higher-frequency modes increased with the sizes of the clusters. For instance, they were $\sim 1100 \text{ cm}^{-1}$, $\sim 1200 \text{ cm}^{-1}$, and $\sim 1400 \text{ cm}^{-1}$ for (LiH)₂, (LiH)₃, and (LiH)₄, respectively. We also compared their geometries, as shown above, and found that the bond distances were 1.758, 1.723, and 1.704 Å for (LiH)₂, (LiH)₃, and (LiH)₄, respectively. Thus, we suggested that the frequencies increased with the size of the clusters, because the bond distances shorten and the bonding was stronger. For the lower-frequency parts, we compared *D*_{4h} with *T_d* geometry in the (LiH)₄ clusters and found that the former had lower frequency (200 cm^{-1}) than the latter (400 cm^{-1}). We suggested that it must be concerned with the single bond rotation and indicated that the chemical bonding of *T_d* geometry was more rigid.

In Table 6, sodium hydride clusters had similar trends. For (NaH)₂ at higher-frequency parts, there were two $\sim 900 \text{ cm}^{-1}$ higher-frequency modes and two $\sim 750 \text{ cm}^{-1}$ lower-frequency modes. For (NaH)₃ at higher-frequency parts, there were three $\sim 1000 \text{ cm}^{-1}$ higher-frequency modes and three $\sim 800 \text{ cm}^{-1}$ lower-frequency modes. For (NaH)₄ at higher-frequency parts, there were four $\sim 1100 \text{ cm}^{-1}$ higher-frequency modes and four $\sim 700 \text{ cm}^{-1}$ lower-frequency modes. In contrast to lithium hydride clusters, we found that sodium hydride clusters had lower frequencies. Same as the lithium hydride clusters, the higher frequencies increased with the size of the clusters. For instance, they were $\sim 900 \text{ cm}^{-1}$, $\sim 1000 \text{ cm}^{-1}$, and $\sim 1100 \text{ cm}^{-1}$ for (NaH)₂, (NaH)₃, and (NaH)₄, respectively. We also compared their geometries, as shown above, and found that the bond distances were 2.119, 2.076, and 2.057 Å for (NaH)₂, (NaH)₃, and (NaH)₄, respectively. Thus, we suggested that the frequencies increased with the size of the clusters, because the bond distances shorten and thus the bonds were stronger. For the lower-frequency parts, we compared *D*_{4h} with *T_d* geometry in the (NaH)₄ clusters and found that the former had a lower frequency (50 cm^{-1}) than the latter (160 cm^{-1}). We suggested that it must be concerned with the single bond rotation and indicated that the chemical bonding of *T_d* geometry was more rigid. From the above analysis, as a result, we suggested that lithium and sodium hydrides had consistent trends, respectively.

In Tables 7 and 8, beryllium and magnesium hydride clusters had some respectively consistent results. But they were not the same as lithium and sodium hydride clusters, which had more regular trends because the environment of each atom in their geometries was not the same. When we compared beryllium

TABLE 7: Frequencies (cm⁻¹) of Beryllium Hydride Clusters at MP2/6-311++G Level**

BeH ₂	(BeH ₂) ₂	(BeH ₂) ₃ (D _{3h})	(BeH ₂) ₃ (chain, C _{2v})	(BeH ₂) ₃ (hat-like, C _{2v})
2284	2199	2170	2188	2193
2069	2178	2157	2182	2182
706	1791	2157	1802	1955
706	1611	2036	1794	1869
	1521	2036	1645	1707
	1485	2017	1645	1472
	962	1352	1546	1401
	723	1344	1511	1360
	601	1344	1464	1245
	566	868	1464	1200
	500	626	906	1120
	332	626	888	1020
		613	888	800
		613	680	799
		609	598	605
		464	598	592
		436	507	554
		436	475	550
		230	475	481
		17	149	419
		17	149	316

(BeH ₂) ₄ (D _{2h})	(BeH ₂) ₄ (T _d)	(BeH ₂) ₄ (C ₁)	(BeH ₂) ₄ (C ₂)
2184	2217	2221	2147
2181	2195	2155	2142
1798	2195	2140	1862
1796	2195	1889	1847
1791	1507	1778	1800
1640	1468	1732	1788
1631	1468	1657	1578
1617	1462	1628	1566
1560	1462	1592	1506
1541	1462	1497	1466
1494	1378	1453	1386
1491	1378	1393	1362
1477	1378	1295	1272
1474	1121	1095	1188
982	1121	975	1102
898	1121	801	1057
888	612	749	767
825	612	716	744
747	612	652	710
724	593	608	703
598	540	565	690
594	540	560	686
487	479	527	636
469	479	503	596
466	479	485	555
389	460	437	509
291	460	421	505
180	460	392	459
100	359	188	405
86	359	118	208

with magnesium hydride clusters, we also found that beryllium hydride clusters had lower frequencies, which is the same as the trends of lithium and sodium hydride clusters.

Summary

We have proven that high-level ab initio molecular orbital theory is certainly used to calculate the geometries, vibrational frequencies, atomic charges, and binding energies of the small clusters (LiH)_n, (NaH)_n, (BeH₂)_n, and (MgH₂)_n (n = 1–4). For (LiH)_n and (NaH)_n, we have found five kinds of structures: C_{∞v}, D_{2h}, D_{3h}, D_{4h}, and T_d. The planar cyclic D_{4h} structure is less stable than the cubic T_d. For (BeH₂)_n and (MgH₂)_n, we have found nine kinds of structures: D_{∞h}, D_{2h}, D_{3h}, hat-like C_{2v}, chain

TABLE 8: Frequencies (cm⁻¹) of Magnesium Hydride Clusters at MP2/6-311++G Level**

MgH ₂	(MgH ₂) ₂	(MgH ₂) ₃ (D _{3h})	(MgH ₂) ₃ (chain, C _{2v})	(MgH ₂) ₃ (hat-like, C _{2v})
1665	1668	1689	1664	1660
1642	1660	1689	1661	1654
446	1342	1654	1354	1482
446	1286	1631	1340	1469
	1150	1631	1298	1269
	1099	1559	1245	1152
	693	957	1158	1026
	379	810	1158	983
	337	810	1097	972
	312	650	1097	943
	304	420	671	843
	230	420	671	761
		375	416	433
		375	352	422
		346	350	377
		271	350	353
		210	284	315
		210	284	305
		169	239	290
		150	65	182
		150	65	180

(MgH ₂) ₄ (D _{2h})	(MgH ₂) ₄ (T _d)	(MgH ₂) ₄ (C ₁)	(MgH ₂) ₄ (C ₂)	(MgH ₂) ₄ (C _{2v})
1662	1687	1687	1633	1822
1661	1675	1636	1631	1780
1350	1675	1626	1423	1780
1348	1675	1463	1423	1664
1338	1197	1418	1415	1652
1307	1197	1374	1396	1638
1290	1197	1359	1204	1638
1218	1178	1270	1161	1636
1158	1178	1173	1157	766
1155	1154	1111	1127	641
1146	977	1071	1122	641
1113	977	980	1016	634
1110	977	920	1010	609
1088	861	843	862	500
685	861	698	860	500
657	861	561	847	367
652	351	513	576	361
446	351	457	525	361
421	351	370	519	310
351	317	346	457	279
350	305	321	347	256
338	305	303	341	256
286	259	299	341	253
285	259	284	331	185
245	259	274	298	125
183	242	233	298	83
108	242	225	294	83
82	242	179	201	69
44	175	92	201	57
37	175	50	86	23

C_{2v}, T_d, C₁, C₂, and chain D_{2h}. (MgH₂)_n has another structure, C_{2v}, when n = 4. The chain C_{2v} and chain D_{2h} structures are more stable than the planar cyclic D_{3h} and cubic T_d when n = 3 and 4, respectively. For the tricentered bonds of the planar cyclic structure, the bond distances shortened as the size of the clusters increased. With the coordinate number increasing, we have found that the bond distances increase as the bond types vary from dicated bonds and tricentered bonds to tetracentered bond. For the atomic charges of these small clusters, it is indicated that the atomic charges of planar cyclic structures are weaker than those of cubic structures. That is, the ionic character increases with the coordinate numbers of atom. For the frequencies of these small clusters, we suggest that the frequencies increase with the size of the clusters because the bond

distances shorten. Eventually, all employed computational methods find the bonding energies to be similar. It is shown that these geometries have converged, and the calculated results must be accurate and reliable.

Acknowledgment. This work is supported in part by the National Science Council of Taiwan, grant no. NSC 93-2113-M194-002. We are grateful to the National Center for High-Performance Computing of Taiwan for providing part of the computational resources.

Supporting Information Available: Cartesian coordinates of small hydride clusters. This material is available free of charge via the Internet at <http://pubs.acs.org>.

Note Added after ASAP Publication. Author Chun-Huei Huang was added and author Wei-Ping Hu was designated as a corresponding author. This paper was published ASAP on 9/22/05 and reposted on 10/10/05.

References and Notes

- (1) Harwood, L. M.; Moody, C. J. *Experimental Organic Chemistry: Principles and Practice*; Blackwell Scientific: Oxford, U.K., 1989.
- (2) Cotton, F.; Wilkinson, G. *Inorganic Chemistry*, 4th ed.; Wiley Interscience: New York, 1980; p 249.
- (3) DeLong, G. T.; Hoffmann, D.; Nguyen, H. D.; Thomas, R. D. *J. Am. Chem. Soc.* **1997**, *119*, 11998.
- (4) Hayward, M. A.; Green, M. A.; Rosseinsky, M. J.; Sloan, J. J. *Am. Chem. Soc.* **1999**, *121*, 8843.
- (5) Yu, R. H.; Schultze, L. M.; Rohloff, J. C.; Dudzinski, P. W.; Kelly, D. E. *Org. Process Res. Dev.* **1999**, *3*, 53.
- (6) Stwalley, W. C.; Zemke, W. T. *J. Phys. Chem. Ref. Data* **1993**, *22*, 87.
- (7) Shukla, A.; Dolg, M.; Stoll, H.; Fulde, P. *Chem. Phys. Lett.* **1996**, *262*, 213.
- (8) Bellaiche, L.; Kunc, K. *Int. J. Quantum Chem.* **1997**, *61*, 647.
- (9) Kulkarni, S. A. *J. Phys. Chem. A* **1998**, *102*, 7704.
- (10) Kulkarni, S. A.; Srivastava, A. K. *J. Phys. Chem. A* **1999**, *103*, 2836.
- (11) Fuentealba, P.; Reyes, O. *J. Phys. Chem. A* **1999**, *103*, 1376.
- (12) Antoine, R.; Dugourd, Ph.; Rayane, D.; Broyer, M. *J. Chem. Phys.* **1996**, *104*, 110.
- (13) Antoine, R.; Dugourd, Ph.; Rayane, D.; Benichou, E.; Broyer, M. *J. Chem. Phys.* **1997**, *107*, 2664.
- (14) Kato, H.; Hirao, K.; Nishida, I.; Kimoto, K. *J. Phys. Chem.* **1981**, *85*, 3391.
- (15) Kollman, P.; Bender, C. E.; Rothenberg, S. *J. Am. Chem. Soc.* **1972**, *94*, 8016.
- (16) Dill, J. D.; Schleyer, P. V. R.; Binkley, J. S.; Pople, J. A. *J. Am. Chem. Soc.* **1977**, *99*, 6159.
- (17) Cardelino, B. H.; Eberhardt, W. H.; Borkman, R. F. *J. Chem. Phys.* **1986**, *84*, 3230.
- (18) Rao, B. K.; Khanna, S. K.; Jena, P. *Phys. Rev. B* **1991**, *43*, 1416.
- (19) Bonačić-Koutecký, V.; Pittner, J.; Koutecký, J. *J. Chem. Phys.* **1996**, *210*, 313.
- (20) Fuentealba, P.; Savin, A. *J. Phys. Chem. A* **2001**, *105*, 11531.
- (21) Abdurahman, A.; Shukla, A.; Dolg, M. *J. Chem. Phys.* **2000**, *112*, 4801.
- (22) Vezin, B.; Dugourd, Ph.; Bordas, C.; Rayane, D.; Broyer, M.; Bonačić-Koutecký, V.; Pittner, J.; Fuchs, C.; Gaus, J.; Koutecký, J. *J. Chem. Phys.* **1995**, *102*, 2727.
- (23) Brendel, G. J.; Marlett, E. M.; Niebyski, L. M. *Inorg. Chem.* **1978**, *17*, 3589.
- (24) Bernath, P. F.; Shayesteh, A.; Tereszchuk, K.; Colin, R. *Science* **2002**, *297*, 1323.
- (25) Szalay, P. G.; Barlett, R. J. *J. Chem. Phys.* **1995**, *103*, 3600.
- (26) Mahapatra, U. S.; Datta, B.; Mukherjee, D. *J. Chem. Phys.* **1999**, *110*, 6171.
- (27) Baer, R.; Neuhauser, D. *J. Chem. Phys.* **2000**, *112*, 1679.
- (28) Martin, J. M. L.; Lee, T. J. *Chem. Phys. Lett.* **1992**, *200*, 502.
- (29) Hehre, W. J.; Radom, L.; Schleyer, P. V. R.; Pople, J. A. *ab initio Molecular Orbital Theory*; John Wiley & Sons: New York, 1986.
- (30) Pople, J. A.; Head-Gordon, M.; Raghavachari, K. *J. Chem. Phys.* **1987**, *87*, 5968.
- (31) Raghavachari, K.; Trucks, G. W.; Pople, J. A.; Head-Gordon, M. *Chem. Phys. Lett.* **1989**, *157*, 479.
- (32) Frisch, M. J.; Trucks, G. W.; Schlegel, H. B.; Scuseria, G. E.; Robb, M. A.; Cheeseman, J. R.; Zakrzewski, V. G.; Montgomery, J. A., Jr.; Stratmann, R. E.; Burant, J. C.; Dapprich, S.; Millam, J. M.; Daniels, A. D.; Kudin, K. N.; Strain, M. C.; Farkas, O.; Tomasi, J.; Barone, V.; Cossi, M.; Cammi, R.; Mennucci, B.; Pomelli, C.; Adamo, C.; Clifford, S.; Ochterski, J.; Petersson, G. A.; Ayala, P. Y.; Cui, Q.; Morokuma, K.; Malick, D. K.; Rabuck, A. D.; Raghavachari, K.; Foresman, J. B.; Cioslowski, J.; Ortiz, J. V.; Stefanov, B. B.; Liu, G.; Liashenko, A.; Piskorz, P.; Komaromi, I.; Gomperts, R.; Martin, R. L.; Fox, D. J.; Keith, T.; Al-Laham, M. A.; Peng, C. Y.; Nanayakkara, A.; Gonzalez, C.; Challacombe, M.; Gill, P. M. W.; Johnson, B. G.; Chen, W.; Wong, M. W.; Andres, J. L.; Head-Gordon, M.; Replogle, E. S.; Pople, J. A. *Gaussian 98*, revision A.7; Gaussian, Inc.: Pittsburgh, PA, 1998.
- (33) Herzberg, G. *Molecular Spectra and Molecular Structure I. Spectra of Diatomic Molecules*, 2nd ed.; Van Nostrand: Princeton, NJ, 1950.
- (34) Atoji, M.; Kikuchi, M. *J. Chem. Phys.* **1970**, *52*, 6434.
- (35) Shull, C. G.; Wollan, E. O.; Morton, G. A.; Davidson, W. L. *Phys. Rev.* **1948**, *73*, 842.
- (36) Ellinger, F. H.; Holley, C. E., Jr.; McInteer, B. B.; Pavone, D.; Potter, R. M.; Staritzky, E.; Zachariassen, W. H. *J. Am. Chem. Soc.* **1955**, *77*, 2647.
- (37) Ahlrichs, R. *Theor. Chim. Acta* **1974**, *35*, 59.
- (38) Rupp, M.; Ahlrichs, R. *Theor. Chim. Acta* **1977**, *46*, 117.